Human Molecular Genetics, 2011, Vol. 20, No. 17 **3331–3345**
doi:10.1093/hmg/ddr239
Advance Access published on May 30, 2011

Pathogenity of some limb girdle muscular dystrophy mutations can result from reduced anchorage to myofibrils and altered stability of calpain 3

Natalia Ermolova[1,3], Elena Kudryashova[1,3], Marino DiFranco[2,3], Julio Vergara[2,3], Irina Kramerova[1,3] and Melissa J. Spencer[1,3,*]

[1]Department of Neurology and [2]Department of Physiology, David Geffen School of Medicine at University of California, Los Angeles, CA 90095, USA and [3]Center for Duchenne Muscular Dystrophy at University of California, Los Angeles, CA 90095, USA

Received March 29, 2011; Revised May 14, 2011; Accepted May 25, 2011

Calpain 3 (CAPN3) is a muscle-specific, calcium-dependent proteinase that is mutated in Limb Girdle Muscle Dystrophy type 2A. Most pathogenic missense mutations in LGMD2A affect CAPN3's proteolytic activity; however, two mutations, D705G and R448H, retain activity but nevertheless cause muscular dystrophy. Previously, we showed that D705G and R448H mutations reduce CAPN3s ability to bind to titin *in vitro*. In this investigation, we tested the consequence of loss of titin binding *in vivo* and examined whether this loss can be an underlying pathogenic mechanism in LGMD2A. To address this question, we created transgenic mice that express R448H or D705G in muscles, on wild-type (WT) CAPN3 or knock-out background. Both mutants were readily expressed in insect cells, but when D705G was expressed in skeletal muscle, it was not stable enough to study. Moreover, the D705G mutation had a dominant negative effect on endogenous CAPN3 when expressed on a WT background. The R448H protein was stably expressed in muscles; however, it was more rapidly degraded in muscle extracts compared with WT CAPN3. Increased degradation of R448H was due to non-cysteine, cellular proteases acting on the autolytic sites of CAPN3, rather than autolysis. Fractionation experiments revealed a significant decrease of R448H from the myofibrillar fraction, likely due to the mutant's inability to bind titin. Our data suggest that R448H and D705G mutations affect both CAPN3s anchorage to titin and its stability. These studies reveal a novel mechanism by which mutations that spare enzymatic activity can still lead to calpainopathy.

INTRODUCTION

Calpain 3 (CAPN3) belongs to a family of Ca^{2+}- activated neutral cysteine proteinases that have been identified in a wide variety of organisms as disparate as humans and worms (1,2). The ability of these thiol proteinases to cleave a wide variety of substrates in response to calcium activation enables their involvement in various cell processes that include cell motility, signal transduction, apoptosis, cell differentiation and regulation of the cytoskeleton (3). In humans, calpains are encoded by 15 genes with the most studied members of the family being the ubiquitously expressed members, calpains 1 and 2, also known as μ- and m-calpain, respectively. These calpains function as a heterodimer, consisting of a large (80 kDa) and a small (28 kDa) subunit (1,4,5). The crystal structure of calpain 2 was resolved in both the apo- and holoenzyme states, providing information on the potential mechanism of activation, which involves autocatalytic cleavage of an N-terminal pro-peptide prior to substrate cleavage (6,7).

Calpain 3 has 54 and 51% sequence homology to the 80 kDa subunits of μ- and m-calpains, respectively, and

*To whom correspondence should be addressed at: 635 Charles Young Drive South, NRB, Room 401, Los Angeles, CA 90095, USA. Tel: +1 3107945225; Fax: +1 3102061998; Email: mspencer@mednet.ucla.edu

shares similar properties with these ubiquitously expressed calpains such as Ca^{2+}- dependent activation and maximal activity at neutral pH (1). At the same time CAPN3 also has distinct characteristics which distinguish it from the ubiquitous calpains (8). First, CAPN3 is predominantly muscle-specific (9), but is detectable in lens, liver, brain and cardiac muscle during development (10–13). Also, CAPN3 lacks a small subunit and likely functions as a homodimer (14–18). CAPN3 has some unique domains including its NH_2-terminal domain I that contains 20–30 additional amino acids not present in μ- and m-calpains and two unique 'insertion sequences' of 62 and 77 amino acids at the COOH-terminal regions of domain II (called IS1) and domain III (called IS2). In addition, the calcium concentration essential for activation is in the nanomolar range (compared with micro and millimolar concentrations for calpain 1 and 2, correspondingly) (19). Finally, CAPN3 is very unstable (18,20) and is subject to fast autoproteolytic degradation, a feature which has made it difficult to thoroughly characterize.

Increased interest in CAPN3 was strongly stimulated when it was reported that mutations in its gene result in limb-girdle muscular dystrophy (LGMD) type 2A, characterized by the gradual atrophy of hip and shoulder muscles (LGMD2A, or calpainopathy) (21). In contrast to other types of muscle dystrophy, where mutations occur in genes encoding structural proteins, calpainopathy was the first reported type of dystrophy predetermined by mutations in a gene encoding a proteolytic enzyme. There are over 440 documented mutations in the calpain 3 gene to date, among them 212 (∼50%) are missense mutations, many of which alter its catalytic activity (22). Since calpains are proteases, pathology is frequently related to impaired catalytic function (21); however, recent studies have exposed a new potential role for CAPN3 as a structural protein (23,24). CAPN3 is a component of the skeletal muscle triad, responsible for calcium release. It is also a component of the dysferlin complex, disruption of which also results in a limb girdle dystrophy (25). It is plausible that the subcellular localization of CAPN3 determines its particular cellular function, and that mutations can affect any of those functions directly or indirectly (1). In addition, the deleterious effect of missense mutations can arise not only from direct disruption of CAPN3 function(s), but also from disruption of the protein's structural integrity, which could affect its intra or intermolecular protein interactions and lead to decreased stability or altered localization. Binding of CAPN3 to titin, a giant myofibrillar protein that serves as a scaffold for sarcomeric proteins, provides an example of such an intermolecular interaction. It has been assumed that titin regulates CAPN3 activity and prevents it from autoproteolytic degradation (8,26).

In this investigation, we aim to gain insight into pathogenic mechanisms underlying the development of calpainopathy. We studied two mutations that do not impact the catalytic activity of CAPN3 (R448H or D705G) but do impact binding to titin (27). For these studies, we created transgenic mice that express these mutated proteins (C3-R448H and C3-D705G) in skeletal muscle lacking endogenous CAPN3, to study the effect of mutant CAPN3 in muscle extracts. These studies demonstrate that at least some mutations that do not affect activity, but impact CAPN3s ability to anchor to titin, are pathogenic. The studies show that the mutations effectively reduce the total concentration of CAPN3 in the myofibrillar fraction by making CAPN3 the target of proteolysis by non-cysteine, cellular proteases.

RESULTS

C3-D705G and C3-R448H retain proteolytic activity

The CAPN3 structure was generated by utilizing protein structure homology modeling using SWISS-MODEL workspace and visualized by PyMol software. The mutated residues R448 and D705 were projected onto the modeled structure. This analysis revealed that both residues are located at a large distance from the active center with R448 being exposed at the surface without obvious contacts with other residues and D705 is located in the EF-hand of domain IV (Fig. 1A). Both observations are consistent with previous reports (28) and suggest that both residues are distant enough from the active center that they should not interfere with proper proteolytic functioning of the enzyme.

To verify this prediction biochemically, we expressed these mutants along with WT (C3-WT) and the active site mutant C129S (C3-C129S) in baculoviral cultures. Western blot analysis of autolytic cleavage was used as an assay of CAPN3 proteolytic function, given that autolysis occurs in three known places in the IS1 domain, resulting in characteristic fragments of 60, 58 and 55 kDa. C3-WT and C3-C129S (proteolytically inactive mutant) were used as positive and negative controls of autocatalytic activity, respectively. The WT protein as well as the three mutant proteins were successfully expressed in the insect cells. The C3-WT, C3-R448H and C3-D705G mutants migrated primarily as the completely cleaved 55 kDa product, with a small amount of protein migrating as 94 kDa (intact CAPN3) (Fig. 1B). As expected, C3-C129S was not degraded and the only band present was the 94 kDa intact CAPN3. Thus, the C3-R448H and C3-D705G mutants showed a cleavage pattern on western blots that is similar to C3-WT and appeared to retain autocatalytic activity.

Creation of transgenic mice expressing mutant calpains on the C3KO background to conduct *in vivo* biochemical studies

We created transgenic mice that express CAPN3 mutants and WT CAPN3 in skeletal muscle to study the biochemical properties of these mutant proteins. Transgenic mice that overexpress mutant cDNAs were created using the human skeletal actin (HSA) promoter to drive expression of R448H and D705G in skeletal muscle. The HSA promoter is activated ∼1 day after birth and does not generally express in cardiac tissue (although some lines are leaky and expression can be detected). These mice were then crossed to the CAPN3 knockout (C3KO) mouse so that the only form of CAPN3 present in the muscles were the mutants: either C3-R448H or C3-D705G.

Protein expression of the transgenes was first analyzed by western blotting of muscles isolated from transgenic mice on both the WT and KO backgrounds. Despite normal expression of CAPN3 mutant proteins in the baculoviral cultures, the C3-D705G mutant protein could not be detected in muscle

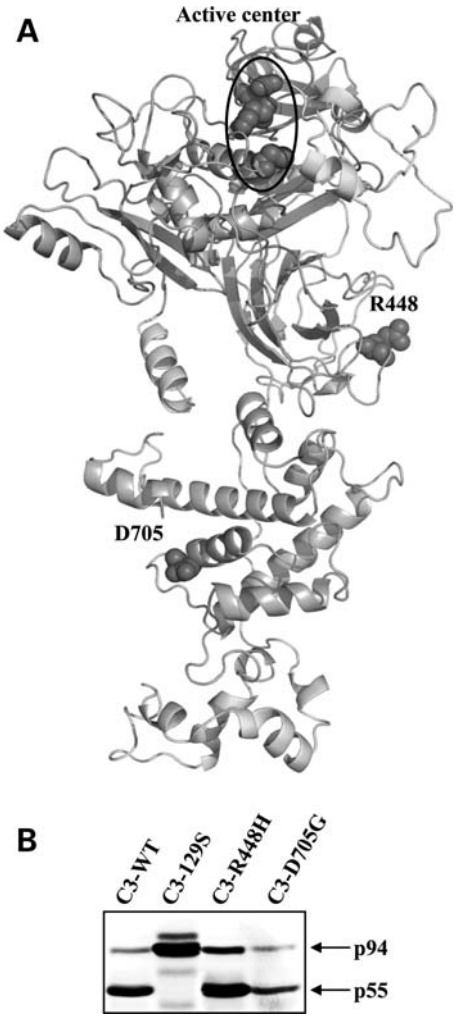

Figure 1. (**A**) Structural model of calpain 3 representing the localization of the active center and residues R448 and D705. A monomer of calpain 3 and its four domains is shown. The active center is circled. R448 is located in domain III facing outward; D705 is located at the 'tip' of EF2 which is one of the calcium-binding EF hands in domain IV. (**B**) Calpain 3 mutants R448H and D705G can be expressed and demonstrate proteolytic activity in baculoviral cultures. Analysis of WT and mutants (C129S-inactive calpain 3; R448H and D705G) expressed in baculoviral cultures and detected using a calpain 3 specific antibody in western blots (the antibody generated against the IS2 domain is a kind gift from Dr Hiro Sorimachi). C129S migrates as a 94 kDa band as expected for a proteolytically inactive mutant. Both D705G and R448H mutants can be expressed in baculoviral cultures and migrate as a cleaved 55 kDa band as would be expected from autolysis in the IS1 domain.

extracts from transgenic mice on the KO background (Fig. 2A). At the same time, results of qPCR of muscle mRNA demonstrated that C3-D705G mRNA was highly expressed in the same muscles (Fig. 2B and C). These findings suggest that loss of C3-D705G mutant protein in muscle extracts is associated with post-transcriptional events, possibly due to rapid degradation of the mutated protein. Moreover, we found that even when the mutant was overexpressed on the WT background (Fig. 2A, lanes Tg+/WT), there was a reduced concentration of the endogenous CAPN3, as if the mutant had a dominant negative influence on the endogenous protein. Since the D705G mutant protein could not be stably expressed, these mice were excluded from further study.

In contrast to C3-D705G, the C3-R448H protein could be detected in muscle extracts, as shown in Figure 3. Moreover, the level of expression of this mutant protein was notably higher than that of endogenous wild-type. Since we were using an overexpression system, mice expressing wild-type CAPN3 were created to use for comparison. We used mice with a similar level of expression (C3-WT) to account for any observations due to overexpression.

Muscles from C3-WT and C3-R448H mice show the same pattern of fiber cross-sectional area distribution

Humans and mice lacking CAPN3 (C3KO) have reduced muscle weight and reduced cross-sectional area of muscle fibers (27). We examined the cross-sectional area of C3-R448H mice to determine if the mutant protein could rescue this aspect of the C3KO phenotype. To resolve this question, cross-sections from soleus muscles of all genotypes of mice (C3-R448H, C3KO and C3-WT and WT mice) were stained for slow myosin (Fig. 4B) and the cross-sectional areas of slow and fast fibers were calculated (Fig. 4A). As expected, the fiber diameter of C3KO was smaller than the fiber diameter in wild-type mice, with the effect more pronounced in fast than in slow fibers. The distribution of fast fiber area for both C3-WT and C3-R448H followed nearly the same pattern as wild-type, with the majority of the fibers in the size range of 1500–2500 μm^2 (Fig. 4A), but C3-WT had more fibers with the larger area. Thus, both mutant and wild-type transgenes could rescue the fast fiber atrophy. The distribution of slow fiber areas for both transgenes was more similar to knock-out muscles than wild-type, with a higher number of the fibers in the size range of 1501–2000 μm^2. Thus, the transgenes were able to rescue the atrophy of fast fibers but not slow fibers. Since the transgene is activated at birth, the observation suggests two possibilities. The first is that CAPN3 plays a role in prenatal growth of slow fibers but does not play a role in growth of slow fibers after birth. This explanation assumes that since the transgene was not activated during fetal growth, the slow fibers were not rescued. Alternatively, it is possible that the expression level was too high in slow fibers and was therefore detrimental in some other manner. If the first possibility is true, then these studies are the first to confirm a role for CAPN3 in developmental aspects of calpainopathy using an *in vivo* model. They also confirm that the C3-R448H transgene is active and able to compensate for the lack of CAPN3 in fast fibers of C3KO muscles.

Muscle strength measurements in calpain 3 transgenes

The results above led to the question of whether the observed rescue of the fast fiber cross sectional area also resulted in a functional improvement in muscle strength in the mice, since the majority of fibers in mouse muscle are of the fast type. To measure strength, we tested the grip strength of transgenic mice and compared with C3KO and WT at five different ages. Results of the grip test for the animals at ages 4 and 6 months of age are shown in Supplementary Material,

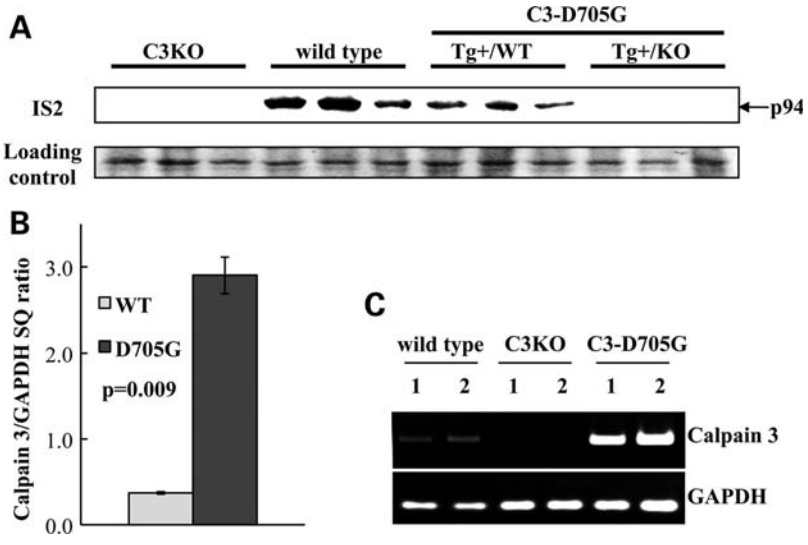

Figure 2. The absence of the D705G mutant protein in muscle extracts is associated with post-transcriptional events. Western blot analysis (**A**), qPCR (**B**) and conventional PCR (**C**) of transgenic skeletal muscle samples from the D705G transgenic mice. (A) Western blot analysis of WT and mutant calpain 3 content in muscle extracts revealed the absence of calpain 3 in C3KO as well as in transgenic positive animals on the C3KO background (Tg+/KO). Note also a dominant negative effect of the D705G transgene on the level of WT CAPN3 in muscle extracts from transgene positive animals on WT background (Tg+/WT). Western blots were done in triplicate for each group of animals. The level of *Capn3* mRNA expression is higher in D705G transgene compared with WT as demonstrated by real-time (B) and conventional (C) PCRs suggesting that the loss of D705G is due to post-transcriptional events. *GAPDH* PCR is used as a cDNA control. Real-time PCR data are shown in graph (B) as the average Starting Quantity (SQ) for *Capn3* normalized by SQ for *GAPDH.* PCR data from two representative samples for each genotype are shown in (C). Vertical bars represent standard error of the mean.

Figure S1. As expected, C3KO mice showed significantly reduced grip strength compared with WT mice. Interestingly, while the wild-type transgene in C3-WT animals was able to rescue the growth defect (Fig. 4A), it did not rescue muscle strength (Supplementary Material, Figure S1), suggesting that these mice are still weak in spite of their larger fiber size. On the contrary, C3-R448H transgenic animals were stronger than wild-types in all age groups tested (data is shown for two representative age groups). This difference in performance between transgenic and control animals was consistent, independent of animal group age, and became more evident in old animals (data not shown). The CAPN3 transgene on the WT background did not affect grip-strength performance (Supplementary Material, Figure S2). Thus, these data suggest that overexpression of active calpain 3 is deleterious to the muscles; and although it positively impacted muscle atrophy, it was not able to rescue the muscle strength. A less stable, but active CAPN3 (C3-R448H) rescued both the growth defect in fast fibers, and the muscle strength. The pathogenicity associated with overexpression of active C3 is consistent with the gatekeeper model proposed by Beckmann and Spencer (29).

Effects of R448H mutation on CAPN3 activity and stability *in vivo*

To determine if C3-WT and C3-R448H transgenes retained proteolytic activity *in vivo*, we assessed their ability to cleave titin, which is an *in vitro* substrate of CAPN3 (30). As titin is an extremely large protein (~3 MDa) and cannot be detected by conventional PAGE, specialized gels optimized for detecting large proteins were run. To demonstrate titin cleavage by CAPN3 *in vivo*, we examined its degradation in wild-type animals compared with C3KO. In Figure 5, the upper band (closed arrowhead) corresponds to intact titin, while the band with a lower molecular weight (open arrowhead) is the product of cleavage by CAPN3. In the absence of CAPN3 (in C3KO muscle), accumulation of the full-length intact titin is apparent. In the presence of active CAPN3, a low-molecular weight fragment is visible on the gel (Fig. 5). Analysis of transgenic muscles revealed that titin was cleaved and the large molecular weight band reduced in both the C3-WT and C3-R448H extracts, verifying that these transgenes are active and able to cleave substrate *in vivo*. Thus, these studies verify titin as an *in vivo* substrate of CAPN3 and confirm the activation of the transgenes.

Previous studies have shown that CAPN3 is much more stable in its native environment of whole muscle than in homogenized muscle extracts (31). It was suggested that this increased stability in whole muscle was due to its anchorage to titin. Our previously published data demonstrated that the R448H mutation reduces CAPN3 binding to titin (30), however, the consequence of this reduced binding on disease and on CAPN3 stability and localization *in vivo* has not been examined. To determine the impact of R448H and disrupted binding to titin on CAPN3's biochemical stability *in vivo*, two sets of experiments were carried out, similar to those performed by Anderson *et al*. (31) on human biopsies. One experiment involved homogenization of fresh muscle tissue (from transgenic animals) in saline and analysis of CAPN3 degradation at various time points. For the second experiment, freshly dissected transgenic muscles were allowed to sit for designated periods of time at room temperature followed by homogenization and western blot analysis of CAPN3 protein. In

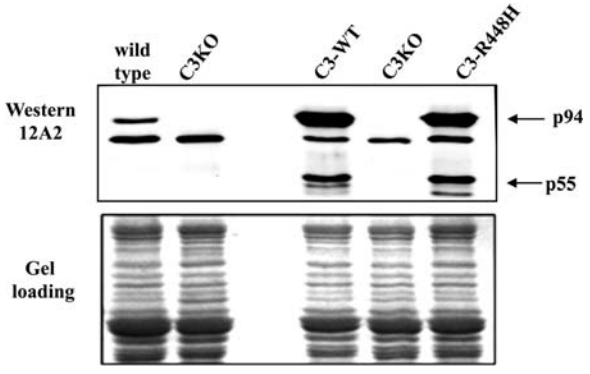

Figure 3. The R448H mutant can be stably expressed in transgenic mouse skeletal muscle. Western blot analysis of muscle extracts from transgenic mice demonstrates that the R448H mutant can be detected *in vivo*. The full length calpain 3 cDNA (C3-WT) was expressed as a transgene to use as a control for the R448H mutant. Characteristic cleavage fragments of 60, 58 and 55 kDa can be seen in extracts from C3-WT and C3-R448H in western blots using the 12A2 antibody.

Figure 6A, it is clearly demonstrated that both C3-WT and C3-R448H underwent fast degradation upon homogenization in saline. However, the rate of C3-R448H degradation was significantly higher than C3-WT (Fig. 6B). Thus, the R448H mutation (and presumably disrupted titin binding) destabilized CAPN3 protein under these conditions.

Whole muscle experiments confirmed previous findings in which CAPN3 was shown to be more stable in whole versus homogenized muscle. In whole muscle, C3-WT showed no significant signs of degradation, even after 30 min of 'sitting' (Fig. 6A). In contrast, C3-R448H was much less stable in whole fresh muscle, where 55% of the protein was degraded after 30 min, migrating as 55–60 kDa degradation fragments on western blot (Fig. 6B). Therefore, both in homogenized muscle and whole muscle, the C3-R448H mutant was much less stable than C3-WT.

C3-R448H is susceptible to proteolytic degradation by cellular proteases in muscle extracts

The observation that the C3-R448H mutant degraded faster than C3-WT led to the hypothesis that this destabilized protein might become the subject of proteolysis by other proteases and not only by autolysis. To test this hypothesis, we used a mixture of non-cysteine proteinase inhibitors (see Methods for details) and carried out biochemical degradation experiments. Muscles from C3-WT and C3-R448H were homogenized in the presence of a protease inhibitor cocktail that had a wide inhibitor spectrum, but did not contain cysteine protease inhibitors, thus preserving CAPN3's autolytic activity. After homogenization, the C3-WT transgene behaved similarly in the absence and presence of protease inhibitors (Fig. 7A, left panel). This observation suggests that most of the proteolytic fragments that were detected in this reaction were a result of autolysis. On the contrary, the rate of C3-R448H degradation was significantly decreased in the presence of inhibitors (Fig. 7A, black dots in R448H graph). Thus, these results suggest the surprising finding that increased lability of the mutant was primarily due to the action of non-cysteine, cellular proteases acting on C3-R448H and not by autolytic degradation. Interestingly, in the presence of inhibitors, the rate of autolysis of C3-R448H, monitored by the appearance of characteristic fragments of 60, 58 and 55 kDa was lower than the rate of C3-WT autolysis. This result suggests that the autocatalytic function of the mutant protein might also be affected by the mutation. Thus, these data show that degradation of the mutant CAPN3 is not through autolysis, but rather proteolysis by other cellular proteases.

To identify the type of protease acting upon C3-R448H, we incubated muscle extracts from the C3-R448H transgenic in the presence of inhibitors of different classes of proteases, each in an individual reaction. As shown in Fig. 7B, all classes of protease inhibitors were effective in preventing some, but not all, of the degradation of the mutant protein. Thus it appears that the R448H mutation results in increased susceptibility to proteolytic degradation by non-cysteine proteases of several different classes. The identification that other cellular proteases can act on the autolytic cleavage sites of CAPN3 is a novel finding and will change the interpretation of many different past and future studies in the area.

Subcellular localization of wild-type CAPN3 and point mutants *in vivo*

We previously showed that R448H and D705G mutants have a reduced ability to bind to titin *in vitro* (30). To study if R448H and D705G mutations cause a relocalization of CAPN3 from the myofibril *in vivo*, we performed two types of experiments. First, we performed *in vivo* electroporation of GFP tagged CAPN3, R448H and D705G mutants in live muscle fibers as described previously (32). A GFP fusion of the active site mutant, C129S was also tested. Numerous studies have attempted to identify the localization of CAPN3 in skeletal muscle by performing immunohistochemistry of tissue sections and isolated myofibrils (33–35). In those studies, CAPN3 was shown to exist in numerous sites including at the N2-line, Z disc, M-line, costameres, nuclei and myotendinous junctions. As an alternative approach and to localize CAPN3 in live muscle, the FDB muscle was electroporated with the GFP-plasmids, and after 3 days, the muscles were dissected and visualized by two-photon laser-scanning microscopy (TPLSM) as previously carried out for other proteins (32,36,37). For these studies, we used two additional indicators as landmarks for the sarcomeric structure: (i) the second harmonic generation (SHG) imaging, which demarcates the A band (myosin thick filaments) and (ii) the staining of a fluorescent non-penetrating potentiometric dye called di-8-ANEPPS, which labels the surface and T-tubule membranes.

Visualization of the active site mutant C3-C129S by TPLSM displayed a double-banded, transverse expression pattern that revealed three peaks per sarcomere (Fig. 8). The peak of the thin C129S band co-localized with the peak of the SHG, which is consistent with M-line localization (Fig. 8, top panel). When compared with di-8-ANEPPS staining, the peaks of the broad C129S bands coincided well with the T-tubules (Fig. 8, bottom panel). C129S was not detected in the nucleus nor at the Z-line, as previously reported by others (33,34). Thus, these data indicate that the active site

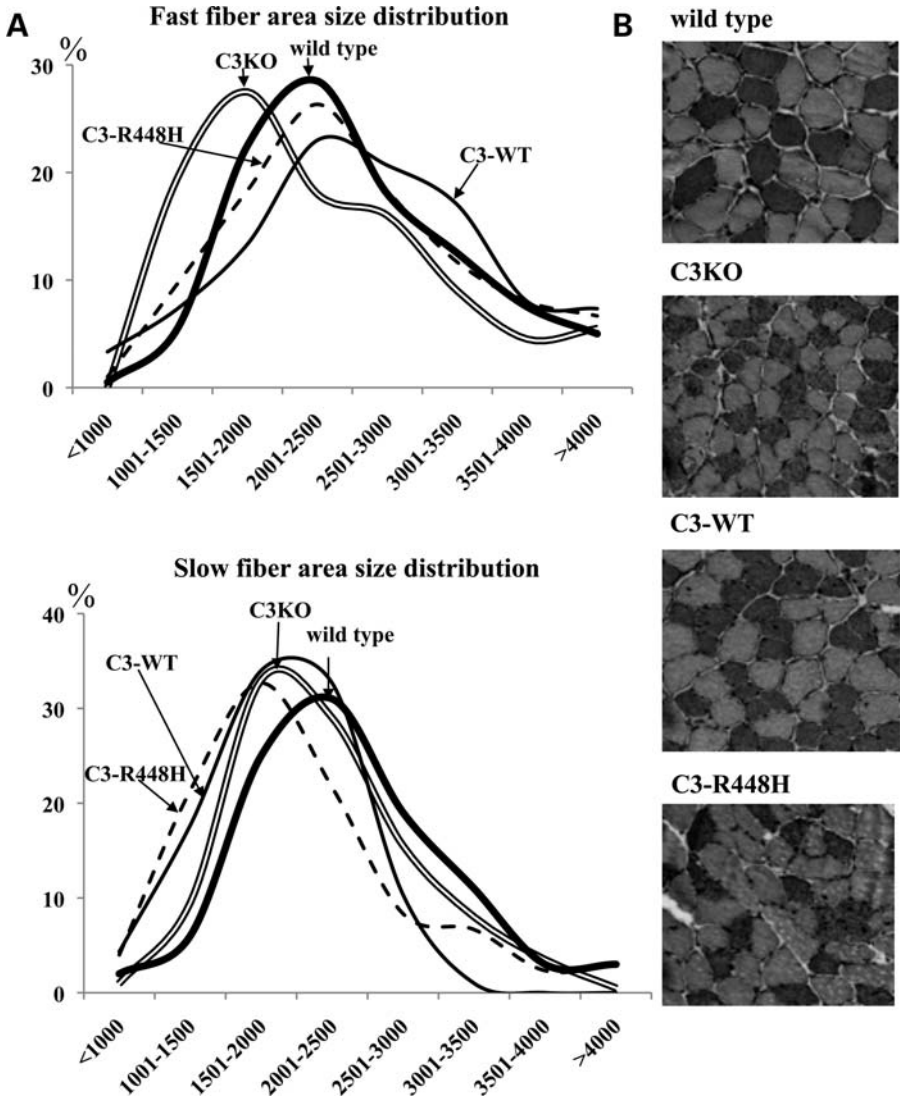

Figure 4. Calpain 3 transgenes rescue the fast fiber atrophy in C3KO, but cannot rescue the slow fiber atrophy. For fiber area size calculations, cross-sections obtained from the mid-belly portion of the soleus muscle (six animals in each group, 10 months old) were stained with monoclonal antibodies to slow myosin heavy chain (**A**). Fast fiber area distribution (top) and slow fiber area distribution (bottom), %. (**B**) Slow myosin immunohistochemical staining of the soleus muscle is shown for all genotypes.

mutant, C129S primarily localizes at the N2-line (as a major band) and at the M-line (as a minor band), supporting its anchorage on titin. This distribution is clearly different from that of soluble GFP (Supplementary Material, Figure S3, top panel), thus ruling out that these findings result from a simple passive distribution of the calpain construct. All other constructs (C3-WT, C3-R448H and C3-D705G) when electroporated, caused destruction of the myofibrillar structure of the muscles, suggesting that CAPN3 is active and harmful for muscles when overexpressed in this manner. Unfortunately, the degraded myofibrils made it impossible to assess the subcellular localization of mutants; however, these experiments constitute the first *in vivo* testing of CAPN3's localization in a muscle fiber and validate previous yeast two-hybrid findings.

As an alternative approach to understanding the effect of mutations on the distribution of CAPN3, we carried out fractionation of transgenic muscle extracts (Fig. 9). As we showed previously (23), CAPN3 is present in the myofibrillar, cytosolic and membrane fractions. Analysis of C3-WT and C3-R448H by western blotting confirmed the established pattern of CAPN3 distribution between these fractions with its highest concentration in cytosolic and myofibrillar fractions. However, densitometric analysis of western blots showed a nearly 3-fold reduction of C3-R448H in the myofibrillar fraction and an ~25% decrease in the membrane fraction compared with C3-WT (Fig. 9). This reduction in C3-R448H content in both fractions likely reflects the effect of the mutation on CAPN3's ability to interact with its binding partner(s) such as titin.

CAPN3 is phosphorylated in the myofibrillar fraction

We employed a structural analysis to investigate how the R448H mutation might impact the secondary structure of

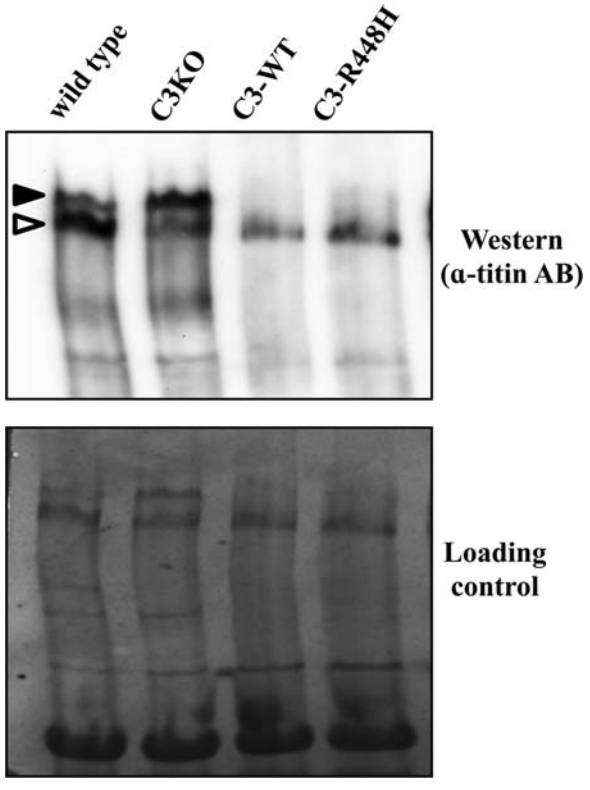

Figure 5. Mutant and WT transgenes retain *in vivo* activity against the CAPN3 substrate titin. Western blot (upper panel) analysis of titin gel (lower panel) revealed two titin bands in WT skeletal muscle: upper band (black arrowhead)—intact titin; lower band (white arrowhead)—cleaved titin fragment. Note accumulation of a cleaved titin fragment in WT skeletal muscle; while on the contrary, intact titin accumulated in C3KO. Both C3-WT and C3-R448H transgenes retained proteolytic activity against their *in vivo* substrate titin.

CAPN3. One of the possibilities we considered was that the mutation affected the secondary structure in such a way that it altered the position of potential salt bridge interacting partners of R448: Asp 452 and Glu 562. Interestingly, both of these acidic residues are surrounded by other residues that could potentially be phosphorylated (Fig. 10A). To verify if the altered structure caused changes in the phosphorylation state of the mutant protein, we compared the phosphorylation state of C3-WT and C3-R448H. The possibility of calpain's 1 and 2 regulation through phosphorylation had been proposed and discussed earlier by Goll *et al*. (1). Initially, we accessed phosphorylation state of calpain 3 immunoprecipitated from whole lysates of C3-WT and C3-R448H transgenic muscles. We were not able to detect phosphorylated CAPN3 in immunoprecipitated material from whole lysates. Most likely the sensitivity of this method is not sufficient to detect such a small percent of phosphorylated protein in the analyzed material (data not shown). Next, we analyzed material immunoprecipitated from the myofibrillar fraction. After isolation of the myofibrillar fraction, CAPN3 was immunoprecipitated and subjected to phosphoprotein analysis. Although the loss of C3-R448H from the myofibrillar fraction made it impossible to determine if differential phosphorylation was taking place between C3-WT and C3-R448H, the data revealed that myofibrillar C3-WT was indeed phosphorylated (Fig. 10B). While further analysis is required to access the phosphorylation state of CAPN3 and its mutants in various fractions, this observation points at phosphorylation as potential regulatory factor for CAPN3 stability, activity or localization. To summarize, our studies showed that the pathogenity of some CAPN3 mutations could be attributed to the loss of CAPN3 anchorage to titin on the myofibril and its degradation by cellular proteases.

DISCUSSION

Mechanisms involved in the pathogenesis of the autosomal recessive LGMD type 2A caused by mutations in the CAPN3 gene (21,38) have been the focus of numerous studies since the identification of the gene defect (reviewed in 1,2). As CAPN3 can serve catalytic or structural functions (23,24) in the cell, depending on its subcellular localization within the muscle fiber, it is feasible that pathogenic mutations can result in alteration of either of these functions. In an attempt to understand which factors might be involved in the development of pathology, we studied two mutations, R448H and D705G, which retain proteolytic activity and are still disease causing. Our previous *in vitro* studies showed that these mutations reduce CAPN3 binding to titin (30). We used an *in vivo* system to perform the ultimate test as to whether mutations that impair calpain anchorage to titin are pathogenic and whether they can affect activity, stability or localization in the muscle environment. Because CAPN3 is more stable *in vivo*, and because we were interested in the effect of these mutations on disease, we developed *in vivo* models to test the question of whether disruption of CAPN3's ability to anchor on titin could be a primary pathogenic mechanism.

Initially, transgenic proteins hosting the R448H or D705G mutations were successfully expressed in a baculoviral system and clearly demonstrated high autolytic activity. The observation that CAPN3 was mainly detected in our recombinant expression system as hydrolyzed fragments is in accordance with previously reported results on high CAPN3 instability when expressed in cell cultures (18,20). Although CAPN3 exhibits fast degradation in muscle homogenates as well, it can be detected in an intact state when examined by western blot immediately after homogenization of fresh muscle (31). It is plausible that CAPN3's ability to withstand degradation in whole muscle can be attributed to stabilizing interactions with some binding partner(s).

Previously reported observations revealed titin as such a partner for CAPN3 (39) as well as an *in vitro* substrate (30). Titin (or connectin) is a huge protein, which spans half the length of the sarcomere (~1 μm) from the M-line to the Z-band. Titin serves as a molecular scaffold for the assembly of sarcomeric proteins and is responsible for passive tension generation within fully differentiated muscle fibers (40,41). It also plays numerous other cellular roles including compartmentalization of metabolic enzymes (binding of DRAL/FHL-2) and positioning of the T-tubules and sarcoplasmic reticulum (binding of sANK1 and obscurin) (42–53). Titin might also act as a stretch sensor that underlies length-dependent signaling processes (54). CAPN3 binds at the N2A and M-line

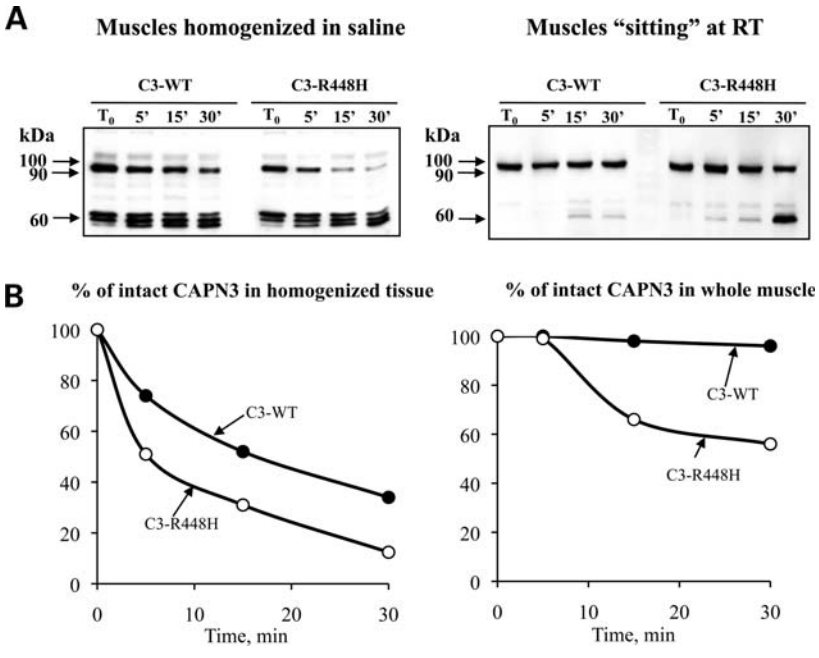

Figure 6. The R448H calpain 3 mutant degrades faster than wild-type calpain 3 in transgenic muscles. (**A**) Western blot analysis of CAPN3 content at different time points in fresh muscles homogenized in saline (left panel) and in whole muscle allowed to 'sit' at room temperature for indicated periods of time (right panel). The calpain 3 specific IS2 antibody was used for detection in western blots. (**B**) Rates of degradation of calpain 3 expressed as a percent of initial concentration of intact protein.

regions of the titin molecule and is able to cleave titin at both the M-line and PEVK region (refer to Supplementary Material, Fig. S4 for schematic representation of CAPN3 localization within myofiber) (26,55). Yeast two-hybrid analysis indicated that binding to the M-line region required the full-length CAPN3 molecule and N2A line binding involved only the IS2 sequence (8,26). It was speculated that localization of CAPN3 in the vicinity of its substrate(s) provides a fast response to changing conditions within the muscle (29).

As previous tests of calpain 3 showed that it is much more stable in its native environment of whole muscle than when the muscle is homogenized (31), it was hypothesized that this increased stability in whole muscle was due to its anchorage on titin and that this association was disrupted by homogenization. Studies here validated a previous report of increased stability of CAPN3 in whole muscle versus homogenized muscle. This observation supports the idea of CAPN3-stabilizing interactions *in vivo*. We tested C3-WT and C3-R448H in both experimental settings and noticed that C3-R448H demonstrated a significantly higher degradation rate than CAPN3 under both conditions. Degradation analysis carried out in the presence of non-cysteine proteinase inhibitors showed that C3-WT was mainly autoproteolyzed and that inhibitors of other cellular proteases did not prevent its autolysis to any significant degree. However, in the case of C3-R448H, degradation by other cellular proteases predominated and was the main reason for the loss of CAPN3 over time. Interestingly, in the presence of the protease inhibitor cocktail, the rate of mutant autolysis was slower than the rate of C3-WT autolysis, meaning that the autocatalytic function of the mutant protein might be affected by the mutation as well as its binding to titin and stability. Despite slowed autocatalytic activity of the C3-R448H compared with C3-WT, both transgenes readily cleaved titin (Fig. 5). These results show that although the mutation does not abolish catalytic activity of CAPN3, it significantly affects the protein's stability.

Proteolytic degradation by cellular proteases may also be the reason why the D705G mutation resulted in loss of CAPN3 protein *in vivo*. Previously, it was shown that C3-D705G binding to titin was lowered *in vitro* (30). Our studies showed that C3-D705G was detectable in the baculoviral culture in active form (Fig. 1B) and the D705G transgene has a dominant-negative effect on endogenous wild-type CAPN3 (Fig. 2A). Notably, the observation of a dominant negative effect fully supports the earlier notions reviewed by Beckmann and Spencer (29) and the dimeric structure proposed for C3 by Davies and colleagues (16). In accord with prior data reported by Davies and colleagues (16), we suggest that CAPN3's ability to bind to titin and its stability are governed by its ability to form a dimer. Thus, it is plausible that the D705G mutant dimerized with endogenous CAPN3 and somehow prevented even WT CAPN3 from binding to titin.

The data demonstrating decreased C3-R448H concentration in the myofibrillar fraction of muscle is consistent with the notion that titin stabilizes and protects CAPN3 from proteolytic and autolytic degradation in the myofibrils. There could be several explanations for this decrease in the amount of C3-R448H bound to titin: (i) given that CAPN3 binds to two different regions of titin, (N2- and M-line) binding to one of those regions could be abated, while binding to the other retained; (ii) alternatively, CAPN3 could retain its ability to bind to both regions, but in this case binding to

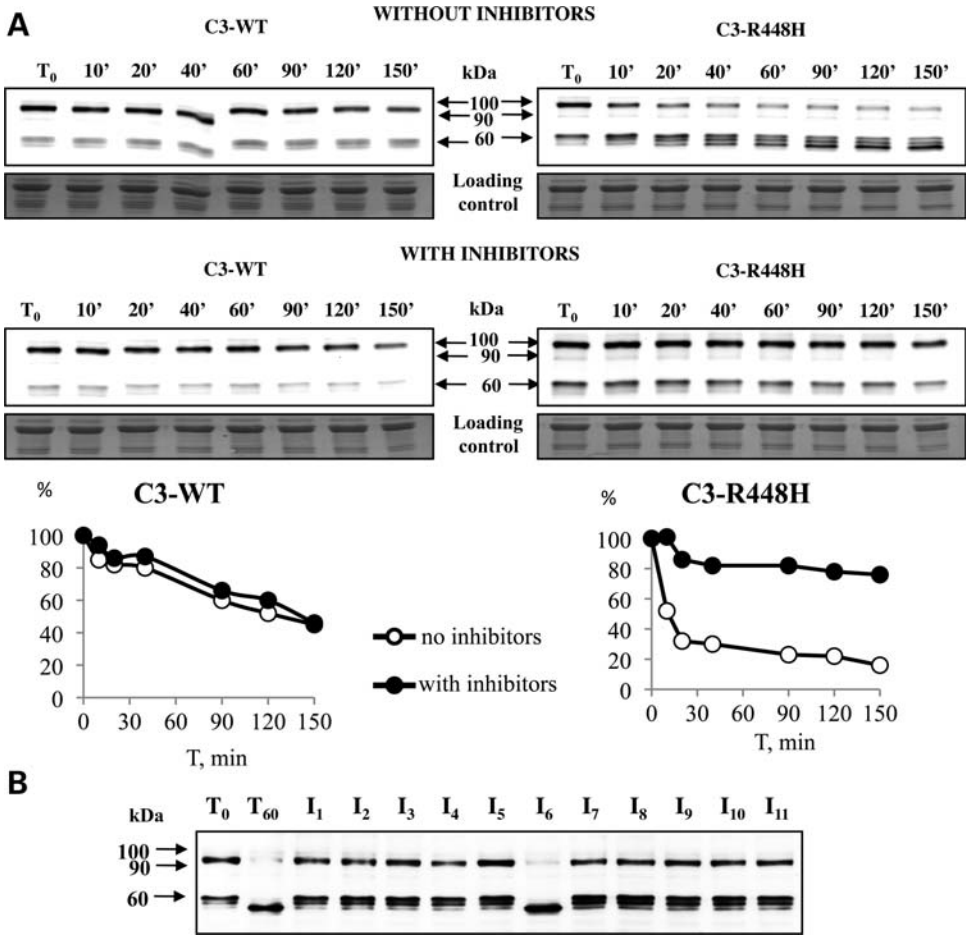

Figure 7. The calpain 3 mutant R448H is rapidly degraded by cellular proteases and not through autolytic degradation. (**A**) Western blot analysis of calpain 3 degradation in the absence and presence of a protease inhibitor cocktail of non-cysteine proteinases (aprotonin, bestatin, pepstatin, AEBSF) shows that degradation of C3-R448H is strongly inhibited, suggesting that the mutation alters protein structure, which makes mutant calpain 3 susceptible to attack from many different cellular proteinases. (**B**) Inhibition of R448H degradation in homogenized muscles by inhibitors targeting individual protease classes. Inhibitors used: I_1-antipain (papain, trypsin, plasmin), I_2-aprotonin (serine proteinases), I_3-bestatin (amino- and exopeptidases), I_4-chymostatin (chymotrypsin), I_5-E64 (cysteine proteinases), I_6-EDTA (metalloproteinases), I_7-leupeptin (serine and cysteine proteinases), I_8-pepstatin (aspartic proteinases), I_9-AEBSF (serine proteinases), I_{10}-phosphoramidon (metalloproteinases), I_{11}-PMSF (serine proteinases). Both experiments were done with frozen muscle samples and probed with the IS2 antibody.

each could be significantly lower; (iii) CAPN3 binds to titin as a dimer and impaired ability of the mutant to dimerize results in reduced binding. Previous *in vitro* experiments showed that although the R448H mutation resulted in a reduction of CAPN3 binding to the titin M-line and N2-line, it did not fully abolish binding to either site (30), so fully abated binding to either site is not likely the case. The two latter reasons may be the likeliest explanation for observed decrease in CAPN3 content.

Previously, it was proposed that CAPN3 might serve its proteolytic function as a dimer formed through the penta-EF-hand domain (16). Recently, it was suggested that dimerization could also occur through domain III as in the case of calpain 8 (56). In the latter situation, oligomerization provides stability rather than a direct affect on proteolytic activity, since both monomer and dimer are active. Based on these reports, we hypothesize that dimer formation could protect the autolytic sites from exposure to the surface and cleavage by cellular proteases and impaired ability of C3-R448H to form a dimer might result in its increased susceptibility to degradation. However, further experiments are required to support this suggestion.

In order to understand the possible impact of the R448H mutation, we used various online tools to analyze its potential consequences. First, we utilized ProPeptide Cleavage Site Prediction server (57) to analyze if any new sites for proteolytic cleavage were formed when the mutation is present. Analysis did not reveal any new cleavage sites. Next we analyzed the structural model of the protein to detect residues in the vicinity of R448 that could be affected by mutations. As such, Glu 562 or Asp 452 could be considered as potential partners for salt bridge formation. Although according to the model those residues are not positioned at an optimal distance for salt bridge formation, potential loop flexibility allows consideration of this assumption. Interestingly, both acidic residues are surrounded by residues which could be potentially phosphorylated (Fig. 10). This notion leads to the hypothesis that if R448 forms a salt bridge with Glu 562 or Asp 452, the

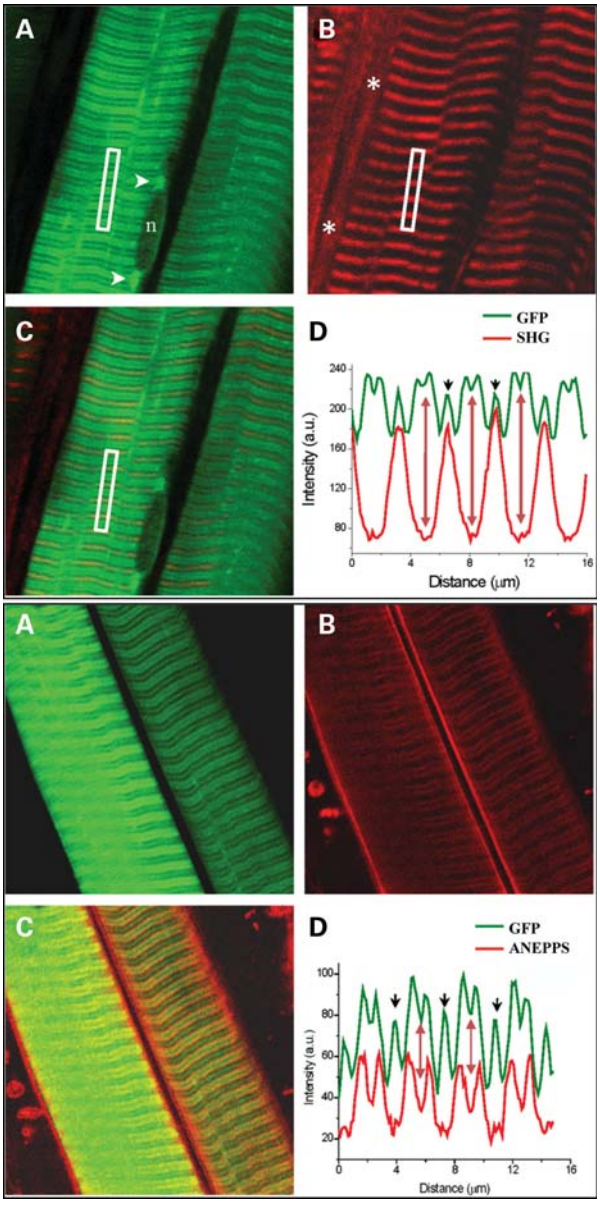

Figure 8. Expression and subcellular localization of GFP-calpain-C129S show co-localization of calpain 3 with the N2 and M line regions of titin. (top panel; versus SHG) (**A** and **B**) TPLSM images of an FDB obtained 3 days after transfection with GFP-calpain-C129S. (A) GFP fluorescence, represented in green tones; **n** is a nucleus and the arrowheads indicate excess fluorescence at the polar regions of the nucleus. (B) Back-scattered second harmonic generation signal, represented arbitrarily by red tones. The asterisks indicate connective tissue. (**C**) Overlay of images shown in (A) and (B). Graph (**D**) represents intensity profiles along the rectangles (16 μm) indicated in A (green trace) and B (red trace). The arrowheads indicate the position of the M lines, and the double-headed arrows indicated the positions of the Z lines. (bottom panel; versus di-8-ANEPPS) (A and B) TPLSM images of an FDB obtained 3 days after transfection with GFP-calpain-C129S, and stained with di-8-ANEPPS prior to imaging. (A) GFP fluorescence, represented in green tones. (B) di-8-ANEPPS fluorescence, represented in red tones. (C) Overlay of images shown in A and B. (**D**) Intensity profiles along the rectangles indicated in A (green trace) and B (red trace). The arrowheads indicate the position of the M-lines, and the double-headed arrows indicated the positions of the Z-lines.

mutation could disrupt this interaction and subsequently affect the phosphorylation state of neighboring residues and/or affect localization of CAPN3. We accessed the phosphorylation state of the C3-WT and C3-R448H transgenes and demonstrated that C3-WT in the myofibrillar fractions is in fact phosphorylated. However, the decreased amount of C3-R448H in the myofibrillar fraction made it impossible to determine if changes in the phosphorylation state coincide with the mutation. Phosphorylation as a factor regulating CAPN3 localization and activity is very attractive, especially if we consider calcium-dependent phosphorylation which could be altered when the mutation is introduced. Notably, domain 3 contains two regions that could be phosphorylated by both CaMKII and CaMKIV (Supplementary Material, Figure S5). R448 is close to the first potential phosphorylation site, which could be affected when the mutation is introduced. It is feasible that CAPN3 binds to titin in a phosphorylated state and phosphorylation stabilizes the protein. The R448H mutation alters this phosphorylation status, thereby altering the structure and exposing sites for proteolytic degradation.

To summarize, these studies demonstrated a correlation between loss of CAPN3-titin binding, loss of CAPN3 from the myofibrillar fraction and reduced stability of CAPN3 in muscle. They are also the first to demonstrate that the 'autolytic' sites in CAPN3 can be cleaved by other cellular proteases. The R448H and D705G mutations likely reduced the stability of CAPN3 by changing the ability of neighboring residue(s) to undergo certain modifications and/or to form stabilizing bonds. The loss of stabilizing bonds could potentially affect dimer formation and/or the phosphorylation state of CAPN3 and, consequently, alter its binding to titin and make it more susceptible to proteolytic degradation by cellular proteases. Although detailed follow-up studies are required to clarify which potential interactions are affected in the case of the R448H mutation, it appears that a proper interaction with titin is abated due to the mutation and that it becomes a target for various proteolytic enzymes. Thus, these studies reveal a novel mechanism by which mutations that do not impact proteolytic activity of CAPN3 enzyme can still be pathogenic.

MATERIALS AND METHODS

Structural modeling

CAPN3 structure was generated by utilizing protein structure homology modeling using SWISS-MODEL workspace (58–60) and visualized by PyMol (URL: The PyMOL Molecular Graphics System, Version 1.2r3pre, Schrödinger, LLC.) and Chimera softwares (http://www.cgl.ucsf.edu/chimera) (61).

Antibodies

Antibodies used for western blot analysis included mouse monoclonal CAPN3 12A2 antibody (1:100), Novocastra; goat polyclonal calpain pIS2 antibody (1:2000) was the generous gift of Dr H. Sorimachi; mouse monoclonal NCL titin antibody (1:750), Novocastra. Secondary Ab anti-mouse and anti-goat conjugates with HRP were from Amersham. Blots were developed using Chemi Glow substrate (Alpha Innotech). Mouse monoclonal slow MHC antibody (1:50), Novocastra, was used for immunohistochemistry.

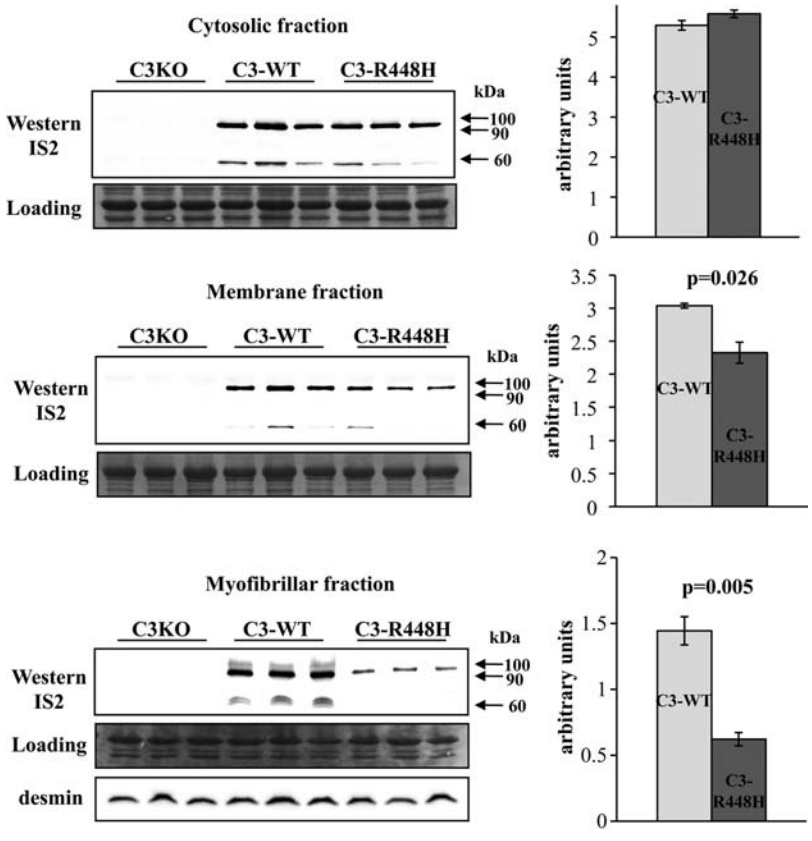

Figure 9. Cellular distribution of calpain 3 among various fractions. Fractionation experiments showed calpain 3 present in myofibrillar, cytosolic and membrane fractions with the highest concentration in cytosolic and myofibrillar fractions for both C3-WT and C3-R448H proteins. The amount of calpain 3 in the myofibrillar and membrane fractions was significantly lower when the R448H mutation was present. Western blots and loading controls are shown to the left of the figure. The corresponding densitometric analysis of western blots is shown to the right. Vertical bars represent standard error of the mean.

Expression of D705G and R448H *in vitro* and *in vivo*

To test whether CAPN3 mutants retain autolytic activity, wild-type CAPN3, C129S, R448H and D705G mutants were cloned into pVL1393 baculoviral transfer vector according to manufacturer's recommendations (BD Biosciences) without any tags to ensure proper protease activity. Insect cells were plated on 10 cm cell-culture dishes at 50–70% of confluence, and infected with CAPN3 high titer viral stocks. After incubation for 3 days at 27°C, cells were harvested by lysis in Insect Cell Lysis Buffer (BD Biosciences) with Protein Inhibitor Cocktail (Sigma, 1:100). Soluble fractions were analyzed by western blotting using anti-CAPN3 antibody to verify CAPN3 expression and to detect the products of autolytic cleavage.

Real-time RT–PCR

Total RNA was isolated from hamstring muscles of wild-type, C3KO and C3-D705G animals using Trizol reagent (Invitrogen) according to manufacturer's protocol. Genomic DNA contamination was removed by DNase treatment for 30 min at 37°C. To produce cDNA, 2 μg of DNA-free RNA was used for first-strand cDNA synthesis with random hexamer primers and Superscript III reverse transcriptase (Invitrogen). The resulting cDNAs were used for PCR amplification of CAPN3 cDNA fragment using the following primers:

sense 5′-CCCACCAGGAGGGGGAATTCATCC-3′ and
antisense 5′- CAGGCCTTGGCTGTGGGGTTTC -3′ (237 bp).

Parallel reactions were run with the same cDNA samples and GAPDH-specific primers:

sense 5′-ACTCCACTCACGGCAAATTC-3′ and
antisense 5′-TCTCCATGGTGGTGAAGACA-3′ (171 bp).

PCR amplification using these primers resulted in the generation of single bands as demonstrated by conventional PCR. All real-time reactions were performed using IQ™ SYBR Green Supermix PCR reagent (Bio-Rad) and My IQ™ Single Color Real-time PCR Detection System (Bio-Rad). Optical System Software Version 1.0 (Bio-Rad) was used to analyze the results. Quantification utilized standard curves made from serial dilutions of control cDNA sample. Data from each sample were normalized by dividing the quantity of target gene cDNA (CAPN3) by the quantity of house-keeping gene cDNA (GAPDH) to correct for variability in the individual samples.

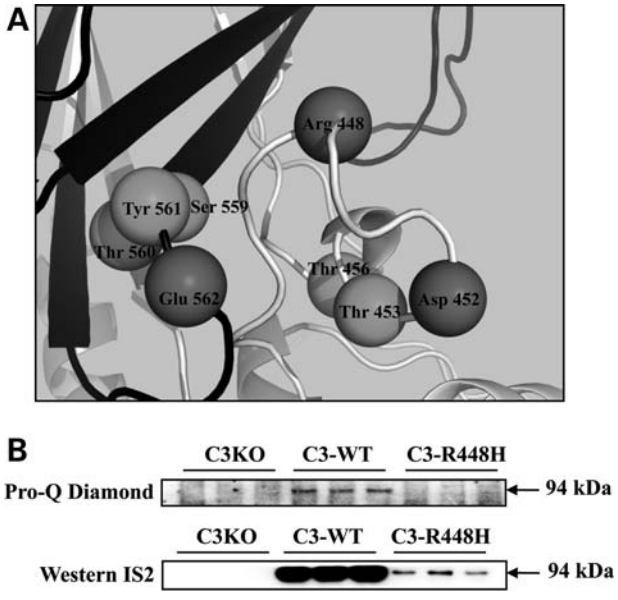

Figure 10. (**A**) Structural analysis of residues in the vicinity of R448. Shown is the structural model of the area surrounding R448. The potential partners of R448 for salt bridge formation are Asp 452 and Glu 562. Both residues are surrounded by amino acids that could be phosphorylated: Thr 453, Thr 456 near Asp 452 and Ser 559, Thr 560, Tyr 561 near Glu 562. (**B**) Detection of phosphorylated calpain 3 in the myofibrillar fraction. Pro-Q Diamond phosphoprotein blot stain was used to assess the phosphorylation state of calpain 3 after immunoprecipitation from solubilized myofibrillar fraction. Phosphorylated calpain 3 was not detected in whole extracts subjected to the same procedure. The phosphoprotein was detected more strongly in the myofibrillar fraction of the mice expressing the wild-type transgene. This result might be due to the loss of C3-R448H from the myofibrillar fraction and not necessarily due to differences in the phosphorylation level of calpain 3; thus, quantitative comparisons could not be made in this experiment. Top panel represents the results of staining immunoprecipitated CAPN3 with pro-Q Diamond for the myofibrillar fraction; lower panel represents the same samples detected with CAPN3 specific IS2 antibody.

Sample preparation and immunoblotting

For expression level analysis, mouse tissues were dissected and frozen in liquid nitrogen. After homogenization on ice in 30 volumes (w/v) of reducing sample buffer [80 mM Tris–HCl (pH 6.8), 2% (w/v) sodium dodecyl sulfate, 10% (v/v) glycerol, 100 mM dithiothreitol and protease inhibitors (P-8340; Sigma-Aldrich)] samples were boiled for 1 min and then centrifuged at 10 000*g* for 5 min at 4°C. Equal amounts of protein (40 μg) were separated by SDS–PAGE and transferred to nitrocellulose membrane (100 V, 1 h, 4°C). CAPN3 content was detected with either 12A2 or IS2 CAPN3 antibody.

For titin electrophoresis, freshly excised gastrocnemius muscles were used. Samples were prepared and analyzed as described previously (62).

Western blot analysis of fresh whole and homogenized in saline quadriceps muscle samples was performed as described by Anderson *et al*. (31). Densitometry was performed utilizing FluorChem FC2 software from Alpha Innotech. CAPN3 content was estimated by IS2 antibody.

Inhibitory analysis with the mixture of non-cysteine inhibitors was performed with frozen quadriceps muscles homogenized on ice in 30 volumes of saline (mg/ml) and immediately divided into two tubes, one of which contained the mixture of aprotonin (serine proteases), bestatin (amino and exo-peptidases), pepstatin (aspartic) and 4-(2-aminoethyl)-benzenesulfonyl-fluoride hydrochloride (AEBSF, serine proteases) at the concentration recommended by the manufacturer (G-Biosciences, cat # 786-207). Equal aliquots were taken after 0, 10, 20, 40, 60, 90, 120 and 150 min of incubation at room temperature and mixed with equal volume of 2× running sample buffer, boiled for 1 min and kept on ice until being analyzed by immunoblotting as described earlier.

Analysis with individual inhibitors was performed as follows: frozen quadriceps muscles were homogenized on ice and immediately transferred to the tubes containing one of the inhibitors listed below and incubated at room temperature for 1 h. Degradation control samples, which did not have inhibitors, were taken immediately after homogenization and after 1 h of incubation. All samples were mixed with 2× running sample buffer, boiled for 1 min and analyzed as described earlier. Inhibitors of various proteases (antipain, aprotonin, bestatin, chymostatin, E64, EDTA, leupeptin, pepstatin, AEBSF, phosphoramidon, PMSF) were used at concentrations recommended by the manufacturer (G-Biosciences, cat # 786-207).

Fractionation

Mouse quadriceps muscles (100–200 mg) from C3KO, C3-WT and C3-R448H (three animals each) were homogenized on ice in 15 volumes of Buffer A (10 mM Tris–HCl, pH 7.8; 0.25 M sucrose, 0.2 mM EDTA), containing phosphatase inhibitors (10 mM sodium fluoride, 10 mM sodium pyrophosphate, 2 mM sodium orthovanadate) and protease inhibitor cocktail (Sigma, cat # P8340). Alternatively, Halt cocktail (ThermoScientific) was used to block protease and phosphatase activity. The homogenates were centrifuged at 2000*g* for 8 min at 4°C. Pellets contained myofibrils, while the supernatant contained mitochondrial, cytosolic and membrane proteins.

The pellets (myofibrillar fraction) were resuspended in the initial volumes of Buffer B (20 mM Tris–HCl, pH 7.2; containing 5 mM EGTA, 100 mM KCl, 1% Triton X-100, phosphatase and protease inhibitors at concentrations mentioned earlier). After incubation on ice for 1 h, the suspension was centrifuged at 3000*g* for 30 min at 4°C. The supernatant was discharged and the pellet was resuspended in the same volume of Buffer B. After centrifugation at 3000*g* for 30 min at 4°C, the pellet was resuspended in 1 ml of Buffer C (20 mM Tris–HCl, pH 7.2; 100 mM KCl and protease/phosphatase inhibitors). DTT was not included in the buffer as it eradicates anti-phosphatase action of sodium orthovanadate. Samples were centrifuged at 3000*g* for 30 min at 4°C, resuspended in Buffer C and filtered through nylon. After centrifugation at 5000*g* for 15 min at 4°C, myofibrils were resuspended in Buffer A and either sonicated for 5 s or passed several times through syringe needle to reduce viscosity.

Supernatant fractions from the first centrifugation step (cytosol, membrane and mitochondria) were centrifuged at 12 000*g* for 15 min at 4°C. Pellets contain mitochondria while supernatants contain cytosolic and membrane proteins.

Mitochondrial fraction was resuspended in Buffer A and subjected for centrifugation at 12 000*g* for 15 min at 4°C repeatedly for 3–4 times. After the last centrifugation, the pellet was snap frozen in liquid nitrogen and kept at −80°C for future analysis.

Cytosolic and membrane fractions were separated by centrifugation at 130 000*g* for 60 min at 4°C. Membrane fraction was dissolved in 0.1–0.2 ml of Buffer A.

All fractions were aliquoted and either mixed with equal amounts of 2× reducing buffer for subsequent PAGE and immunoblotting or frozen in liquid nitrogen and kept at −80°C for future use.

Phosphorylation status of CAPN3 transgenes in myofibrillar fraction was analyzed following fractionation and immunoprecipitation with IS2 antibody by Pro-Q Diamond phosphoprotein blot staining (Molecular probes). The same membrane was analyzed for CAPN3 content after removal of phosphoprotein stain. In addition, samples were tested with anti-phosphotyrosine antibody (Cell Signaling).

Immunohistochemistry

Muscles to be used for immunohistochemistry were dissected from the mice and frozen in isopentane cooled in liquid nitrogen. Frozen muscles were cross-sectioned mid-belly at 10 μm and kept frozen until use. For fiber area size distribution, sections obtained from the soleus muscle of six animals in each group were stained with monoclonal antibodies to myosin heavy chain (slow type, 1:50, Novacastra). After thawing, sections were treated with 0.3% H_2O_2 for 5 min (if horseradish peroxidase was used for color reaction) and blocked in phosphate-buffered saline (PBS) with 0.2% gelatin, 0.5% Tween-20 and 3% bovine serum albumin for 30 min. Binding to endogenous mouse IgG was blocked with a MOM Kit (Vector Laboratories). After primary and biotin-conjugated secondary antibodies, sections were incubated with avidin-conjugated horseradish peroxidase and stained using AEC substrate kit (Vector Laboratories). Slides were mounted in Gel/Mount (Biomed Corp.) and examined under a Zeiss microscope.

Muscle transfection with GFP construct and TPLSM

Lower limb foot pad muscles of 3-month-old C57BL male mice were transfected with GFP fusions of CAPN3, C129S (active site mutant), R448H and D705G by *in vivo* electroporation as previously described (36) and examined by TPLSM to elucidate the subcellular localization of CAPN3 and the effect of mutations on localization. GFP alone was used as a negative control. Male C57BL (3 months old) were used for transfection. Muscles were dissected 3 days after transfection. FDB and interossei muscles were dissected and cleaned from connective tissue. Muscles were stretched about 50% above slack length, pinned down to small Petri dished layered with Sylgard and bathed in Tyrode. Distribution of GFP and its fusions were determined by comparing the GFP fluorescence pattern with the fluorescence intensity of SHG and di-8-ANEPPS, specific markers of the M-line and the T-tubules, respectively. GFP and di-8-ANEPPS were excited at 890 nm, and their emission was collected at 515–555 and 600–645 nm, respectively. Back-scattered SGH was collected at 420–460 nm. Images were acquired with a commercial TPLSM composed of an upright microscope (Olympus), a BioRad scanning head and detection system (Radiance 2000, Zeiss/BioRad) and a Ti-Shapire laser (Chameleon, Coherent). A 20×, 0.95NA, water immersion objective was used (Olympus). Images were analyzed using public domain software ImageJ and MicroCal Origin.

Fiber area size distribution

Fiber cross-sectional area was measured for 150–300 individual fibers in cross-sections of gastrocnemius muscles from each of six WT, C3KO, C3-WT and C3-R448H animals. Sections were stained with anti-slow MHC antibodies as described earlier and slow and fast twitch muscle area were measured separately using a digitized imaging system (Bioquant, Nashville, TN, USA).

Functional test

Forelimb grip strength was measured using a digital force gauge (DFIS 2, Chatillon CE). In each trial, the mouse was allowed to grasp a metal rod and the technician slowly pulled the mouse by the tail until the digital gauge recorded the peak tension (in Newtons) produced. Five trials were performed with a minimum of 1 min rest in between. Upon completion of the grip strength test, the body weight was recorded. For analysis, peak tension produced in all five trials was averaged and normalized for body weight.

All experimental protocols and use of animals were conducted in accordance with the National Institute of Health Guide for Care and Use of Laboratory Animals and approved by the UCLA Institutional Animal Care and Use Committee.

SUPPLEMENTARY MATERIAL

Supplementary Material is available at *HMG* online.

ACKNOWLEDGEMENTS

The authors would like to thank Jane Wen and Leonel Martinez for excellent technical assistance. The transgenic mice used in this investigation were generated at the University of California, Irvine, Transgenic mouse facility. The authors thank Dr T. Otis, Department of Neurobiology, UCLA, for the shared use of the TPLSM system.

Conflict of Interest statement. None declared.

FUNDING

This work was supported by grants from the National Institutes of Health (NIAMS) (5R01AR048177, 5R01AR052693 and 5P30AR057230 to M.S., AR047664, AR041802 and AR054816 to J.V.); and the Muscular Dystrophy Association of America to M.S.

REFERENCES

1. Goll, D.E., Thompson, V.F., Li, H., Wei, W. and Cong, J. (2003) The calpain system. *Physiol. Rev.*, **83**, 731–801.
2. Sorimachi, H., Hata, S. and Ono, Y. (2010) Expanding members and roles of the calpain superfamily and their genetically modified animals. *Exp. Anim.*, **59**, 549–566.
3. Croall, D.E. and Ersfeld, K. (2007) The calpains: modular designs and functional diversity. *Genome Biol.*, **8**, 218.
4. Sorimachi, H. and Suzuki, K. (2001) The structure of calpain. *J. Biochem.*, **129**, 653–664.
5. Suzuki, K., Sorimachi, H., Yoshizawa, T., Kinbara, K. and Ishiura, S. (1995) Calpain: novel family members, activation, and physiologic function. *Biol. Chem. Hoppe Seyler*, **376**, 523–529.
6. Hanna, R.A., Campbell, R.L. and Davies, P.L. (2008) Calcium-bound structure of calpain and its mechanism of inhibition by calpastatin. *Nature*, **456**, 409–412.
7. Jia, Z., Hosfield, C.M., Davies, P.L. and Elce, J.S. (2002) Crystal structure of calpain and insights into Ca(2+)-dependent activation. *Meth. Mol. Biol.*, **172**, 51–67.
8. Sorimachi, H., Kinbara, K., Kimura, S., Takahashi, M., Ishiura, S., Sasagawa, N., Sorimachi, N., Shimada, H., Tagawa, K., Maruyama, K. *et al.* (1995) Muscle-specific calpain, p94, responsible for limb girdle muscular dystrophy type 2A, associates with connectin through IS2, a p94-specific sequence. *J. Biol. Chem.*, **270**, 31158–31162.
9. Sorimachi, H., Imajoh, O.S., Emori, Y., Kawasaki, H., Ohno, S., Minami, Y. and Suzuki, K. (1989) Molecular cloning of a novel mammalian calcium-dependent protease distinct from both m- and mu-types. Specific expression of the mRNA in skeletal muscle. *J. Biol. Chem.*, **264**, 20106–20111.
10. Poussard, S., Duvert, M., Balcerzak, D., Ramassamy, S., Brustis, J.J., Cottin, P. and Ducastaing, A. (1996) Evidence for implication of muscle-specific calpain (p94) in myofibrillar integrity. *Cell Growth Differ.*, **7**, 1461–1469.
11. Konig, N., Raynaud, F., Feane, H., Durand, M., Mestre-Frances, N., Rossel, M., Ouali, A. and Benyamin, Y. (2003) Calpain 3 is expressed in astrocytes of rat and Microcebus brain. *J. Chem. Neuroanat.*, **25**, 129–136.
12. Ma, H., Fukiage, C., Azuma, M. and Shearer, T.R. (1998) Cloning and expression of mRNA for calpain Lp82 from rat lens: splice variant of p94. *Invest. Opthalmol. Vis. Sci.*, **39**, 454–461.
13. Fougerousse, G., Durand, M., Suel, L., Pourquie, O., Delezoide, A., Romero, N.B., Abitbol, M. and Beckmann, J.S. (1998) Expression of Genes (CAPN3, SGCA, SGCB, AND TTN) involved in progressive muscular dystrophies during early human development. *Genomics*, **48**, 145–156.
14. Blanchard, H., Li, Y., Cygler, M., Kay, C.M., Simon, J., Arthur, C., Davies, P.L. and Elce, J.S. (1996) Ca(2+)-binding domain VI of rat calpain is a homodimer in solution: hydrodynamic, crystallization and preliminary X-ray diffraction studies. *Pr. Sci.*, **5**, 535–537.
15. Blanchard, H., Grochulski, P., Li, Y., Arthur, J.S., Davies, P.L., Elce, J.S. and Cygler, M. (1997) Structure of a calpain Ca(2+)-binding domain reveals a novel EF-hand and Ca(2+)-induced conformational changes. *Nat. Struct. Biol.*, **4**, 532–538.
16. Ravulapalli, R., Diaz, B.G., Campbell, R.L. and Davies, P.L. (2005) Homodimerization of calpain 3 penta-EF-hand domain. *Biochem. J.*, **388**, 585–591.
17. Ravulapalli, R., Campbell, R.L., Gauthier, S.Y., Dhe-Paganon, S. and Davies, P.L. (2009) Distinguishing between calpain heterodimerization and homodimerization. *Febs. J.*, **276**, 973–982.
18. Kinbara, K., Ishiura, S., Tomioka, S., Sorimachi, H., Jeong, S.Y., Amano, S., Kawasaki, H., Kolmerer, B., Kimura, S., Labeit, S. *et al.* (1998) Purification of native p94, a muscle-specific calpain, and characterization of its autolysis. *Biochem. J.*, **335**, 589–596.
19. Garcia Diaz, B.E., Gauthier, S. and Davies, P.L. (2006) Ca2+ dependency of calpain 3 (p94) activation. *Biochemistry*, **45**, 3714–3722.
20. Sorimachi, H., Toyama-Sorimachi, N., Saido, T.C., Kawasaki, H., Sugita, H., Miyasaka, M., Arahata, K., Ishiura, S. and Suzuki, K. (1993) Muscle-specific calpain, p94, is degraded by autolysis immediately after translation, resulting in disappearance from muscle. *J. Biol. Chem.*, **268**, 10593–10605.
21. Richard, I., Broux, O., Allamand, V., Fougerousse, F., Chiannilkulchai, N., Bourg, N., Brenguier, L., Devaud, C., Pasturaud, P., Roudaut, C. *et al.* (1995) Mutations in the proteolytic enzyme calpain 3 cause limb-girdle muscular dystrophy type 2A. *Cell*, **81**, 27–40.
22. Garnham, C.P., Hanna, R.A., Chou, J.S., Low, K.E., Gourlay, K., Campbell, R.L., Beckmann, J.S. and Davies, P.L. (2009) Limb-girdle muscular dystrophy type 2A can result from accelerated autoproteolytic inactivation of calpain 3. *Biochemistry*, **48**, 3457–3467.
23. Kramerova, I., Kudryashova, E., Wu, B., Ottenheijm, C., Granzier, H. and Spencer, M.J. (2008) Novel Role For Calpain-3 In The Triad-Associated Protein Complex Regulating Calcium Release In Skeletal Muscle. *Hum. Mol. Genet.*, **17**, 3271–3280.
24. Ojima, K., Ono, Y., Ottenheijm, C., Hata, S., Suzuki, H., Granzier, H. and Sorimachi, H. (2011) Non-proteolytic functions of calpain-3 in sarcoplasmic reticulum in skeletal muscles. *J. Mol. Biol.*, **407**, 439–449.
25. Kramerova, I., Beckmann, J.S. and Spencer, M.J. (2007) Molecular and cellular basis of calpainopathy (limb girdle muscular dystrophy type 2A). *Biochim. Biophys. Acta*, **1772**, 128–144.
26. Kinbara, K., Sorimachi, H., Ishiura, S. and Suzuki, K. (1997) Muscle-specific calpain, p94, interacts with the extreme C-terminal region of connectin, a unique region flanked by two immunoglobulin C2 motifs. *Arch. Biochem. Biophys.*, **342**, 99–107.
27. Zou, P., Pinotsis, N., Lange, S., Song, Y.H., Popov, A., Mavridis, I., Mayans, O.M., Gautel, M. and Wilmanns, M. (2006) Palindromic assembly of the giant muscle protein titin in the sarcomeric Z-disk. *Nature*, **439**, 229–233.
28. Jia, Z., Petrounevitch, V., Wong, A., Moldoveanu, T., Davies, P.L., Elce, J.S. and Beckmann, J.S. (2001) Mutations in calpain 3 associated with limb girdle muscular dystrophy: analysis by molecular modeling and by mutation in m-calpain. *Biophys. J.*, **80**, 2590–2596.
29. Beckmann, J.S. and Spencer, M. (2008) Calpain 3, the "gatekeeper" of proper sarcomere assembly, turnover and maintenance. *Neuromusc. disorders: NMD*, **18**, 913–921.
30. Kramerova, I., Kudryashova, E., Tidball, J.G. and Spencer, M.J. (2004) Null mutation of calpain 3 (p94) in mice causes abnormal sarcomere formation in vivo and in vitro. *Hum. Mol. Gen.*, **13**, 1373–1388.
31. Anderson, L.V., Davison, K., Moss, J.A., Richard, I., Fardeau, M., Tomé, F.M., Hübner, C., Lasa, A., Colomer, J. and Beckmann, J.S. (1998) Characterization of monoclonal antibodies to calpain 3 and protein expression in muscle from patients with limb-girdle muscular dystrophy type 2A. *Am. J. Path.*, **153**, 1169–1179.
32. DiFranco, M., Neco, P., Capote, J., Meera, P. and Vergara, J.L. (2006) Quantitative evaluation of mammalian skeletal muscle as a heterologous protein expression system. *Prot. Expr. Purif.*, **47**, 281–288.
33. Keira, Y., Noguchi, S., Minami, N., Hayashi, Y.K. and Nishino, I. (2003) Localization of calpain 3 in human skeletal muscle and its alteration in limb-girdle muscular dystrophy 2A muscle. *J. Biochem. (Tokyo)*, **133**, 659–664.
34. Baghdiguian, S., Martin, M., Richard, I., Pons, F., Astier, C., Bourg, N., Hay, R.T., Chemaly, R., Halaby, G., Loiselet, J. *et al.* (1999) Calpain 3 deficiency is associated with myonuclear apoptosis and profound perturbation of the IkappaB alpha/NF-kappaB pathway in limb-girdle muscular dystrophy type 2A. *Nat. Med.*, **5**, 503–511.
35. Taveau, M., Bourg, N., Sillon, G., Roudaut, C., Bartoli, M. and Richard, I. (2003) Calpain 3 is activated through autolysis within the active site and lyses sarcomeric and sarcolemmal components. *Mol. Cell Biol.*, **23**, 9127–9135.
36. DiFranco, M., Quinonez, M., Capote, J. and Vergara, J. (2009) DNA transfection of mammalian skeletal muscles using in vivo electroporation. *J. Vis. Exp.*, **32**, 1–11.
37. DiFranco, M., Tran, P., Quinonez, M. and Vergara, J.L. (2011) Functional Expression of Transgenic 1sDHPR Channels in Adult Mammalian Skeletal Muscle Fibers. *J. Physiol.*, **589**, 1421–1442.
38. Spencer, M.J., Tidball, J.G., Anderson, L.V., Bushby, K.M., Harris, J.B., Passos-Bueno, M.R., Somer, H., Vainzof, M. and Zatz, M. (1997) Absence of calpain 3 in a form of limb-girdle muscular dystrophy (LGMD2A). *J. Neurol. Sci.*, **146**, 173–178.
39. Sorimachi, H., Ono, Y. and Suzuki, K. (2000) Skeletal muscle-specific calpain, p94, and connectin/titin: their physiological functions and relationship to limb-girdle muscular dystrophy type 2A. *Adv. Exp. Med. Biol.*, **481**, 383–387.
40. Granzier, H. and Labeit, S. (2007) Structure-function relations of the giant elastic protein titin in striated and smooth muscle cells. *Muscle Nerve*, **36**, 740–755.

41. Tskhovrebova, L. and Trinick, J. (2010) Roles of titin in the structure and elasticity of the sarcomere. *J. Biomed. Biotechnol.*, **2010**:612482.
42. Garvey, S.M., Rajan, C., Lerner, A.P., Frankel, W.N. and Cox, G.A. (2002) The muscular dystrophy with myositis (mdm) mouse mutation disrupts a skeletal muscle-specific domain of titin. *Genomics*, **79**, 146–149.
43. Haravuori, H., Vihola, A., Straub, V., Auranen, M., Richard, I., Marchand, S., Voit, T., Labeit, S., Somer, H., Peltonen, L. *et al.* (2001) Secondary calpain3 deficiency in 2q-linked muscular dystrophy: titin is the candidate gene. *Neurology*, **56**, 869–877.
44. Kellermayer, M.S. and Granzier, H.L. (1996) Elastic properties of single titin molecules made visible through fluorescent F-actin binding. *Biochem. Biophys. Res. Comm.*, **221**, 491–497.
45. Labeit, S. and Kolmerer, B. (1995) Titins: giant proteins in charge of muscle ultrastructure and elasticity. *Science*, **270**, 293–296.
46. Radke, M.H., Peng, J., Wu, Y., McNabb, M., Nelson, O.L., Granzier, H. and Gotthardt, M. (2007) Targeted deletion of titin N2B region leads to diastolic dysfunction and cardiac atrophy. *PNAS*, **104**, 3444–3449.
47. Trinick, J. and Tskhovrebova, L. (1999) Titin: a molecular control freak. *Trends Cell Biol.*, **9**, 377–380.
48. Trombitás, K., Greaser, M., French, G. and Granzier, H. (1998) PEVK extension of human soleus muscle titin revealed by immunolabeling with the anti-titin antibody 9D10. *J. Struct. Biol.*, **122**, 188–196.
49. Tskhovrebova, L. and Trinick, J. (2003) Titin: properties and family relationships. *Nat. Rev. Mol. Cell Biol.*, **4**, 679–689.
50. Wu, Y., Labeit, S., Lewinter, M.M. and Granzier, H. (2002) Titin: an endosarcomeric protein that modulates myocardial stiffness in DCM. *J. Card. Fail.*, **8**, S276–S286.
51. Maiweilidan, Y., Klauza, I. and Kordeli, E. (2011) Novel interactions of ankyrins-G at the costameres: the muscle-specific Obscurin/Titin-related-Binding Domain (OTBD) binds plectin and filamin C. *Exp. Cell Res.*, **317**, 724–736.
52. Gautel, M. (2010) The sarcomeric cytoskeleton: who picks up the strain? *Curr. Opin. Cell Biol.*, **23**, 39–46.
53. Bagnato, P., Barone, V., Giacomello, E., Rossi, D. and Sorrentino, V. (2003) Binding of an ankyrin-1 isoform to obscurin suggests a molecular link between the sarcoplasmic reticulum and myofibrils in striated muscles. *J. Cell Biol.*, **160**, 245–253.
54. Linke, W.A. (2008) Sense and stretchability: the role of titin and titin-associated proteins in myocardial stress-sensing and mechanical dysfunction. *Cardiovasc. Res.*, **77**, 637–648.
55. Hayashi, C., Ono, Y., Doi, N., Kitamura, F., Tagami, M., Mineki, R., Arai, T., Taguchi, H., Yanagida, M., Hirner, S. *et al.* (2008) Multiple molecular interactions implicate the connectin/titin N2A region as a modulating scaffold for p94/calpain 3 activity in skeletal muscle. *J. Biol. Chem.*, **283**, 14801–14814.
56. Hata, S. and Sorimachi, H. (2007) New biology of calpain in relation with intracellular membrane systems. *Seikagaku*, **79**, 46–50.
57. Duckert, P., Brunak, S. and Blom, N. (2004) Prediction of proprotein convertase cleavage sites. *Pr. Eng. Des. Sel.*, **17**, 107–112.
58. Arnold, K., Bordoli, L., Kopp, J. and Schwede, T. (2006) The SWISS-MODEL workspace: a web-based environment for protein structure homology modelling. *Bioinformatics*, **22**, 195–201.
59. Kiefer, F., Arnold, K., Kunzli, M., Bordoli, L. and Schwede, T. (2009) The SWISS-MODEL Repository and associated resources. *Nucleic Acids Res.*, **37**, D387–D392.
60. Peitsch, M.C., Wells, T.N., Stampf, D.R. and Sussman, J.L. (1995) The Swiss-3D Image collection and PDB-Browser on the World-Wide Web. *Trends Biochem. Sci.*, **20**, 82–84.
61. Pettersen, E.F., Goddard, T.D., Huang, C.C., Couch, G.S., Greenblatt, D.M., Meng, E.C. and Ferrin, T.E. (2004) UCSF Chimera–a visualization system for exploratory research and analysis. *J. Comput. Chem.*, **25**, 1605–1612.
62. Huebsch, K.A., Kudryashova, E., Wooley, C.M., Sher, R.B., Seburn, K.L., Spencer, M.J. and Cox, G.A. (2005) Mdm muscular dystrophy: interactions with calpain 3 and a novel functional role for titin's N2A domain. *Hum. Mol. Gen.*, **14**, 2801–2811.